

## Cross-Section Ratios of Isomeric Nuclides Produced in Medium-Energy ( $\alpha, xn$ ) Reactions\*

T. MATSUO,† J. M. MATUSZEK,‡ JR., N. D. DUDEY,§ AND T. T. SUGIHARA

Clark University, Worcester, Massachusetts

(Received 29 March 1965)

Cross-section ratios of isomeric nuclides produced in the reactions  $^{41}\text{K}(\alpha, n)^{44}\text{Sc}$ ,  $^{55}\text{Mn}(\alpha, n)^{58}\text{Co}$ ,  $^{93}\text{Nb}(\alpha, n)^{96}\text{Tc}$ ,  $^{93}\text{Nb}(\alpha, 2n)^{95}\text{Tc}$ ,  $^{93}\text{Nb}(\alpha, 3n)^{94}\text{Tc}$ , and  $^{136}\text{Ba}(\alpha, 3n)^{137}\text{Ce}$  are reported for the  $\alpha$ -particle energy range from reaction threshold to 42 MeV. Recoil ranges of products were also determined. Range information was used to help establish the bombarding-energy region in which a particular reaction was likely to be compound-nuclear. The ratio of cross sections, high-spin product to low-spin product, was found to increase initially as the bombarding energy increased. In the three ( $\alpha, n$ ) reactions, the ratio goes through a maximum and decreases. The decreasing region is consistent with the onset of a process in which the product nucleus does not have all of the momentum of the incident  $\alpha$  particle. In the  $^{93}\text{Nb}(\alpha, 2n)$  reaction the cross-section ratio also goes through a maximum, but the range measurements in this energy region suggest that in only a small fraction of events is the momentum transfer much less than complete. Both ( $\alpha, 3n$ ) reactions show a monotonic increase in the cross-section ratio with increasing  $\alpha$ -particle energy. Excitation functions of isomeric pairs indicate a shift to higher bombarding energy for the nuclide of higher spin.

### I. INTRODUCTION

NUCLEAR reactions in the medium-energy region (<50 MeV excitation) have been studied in a variety of ways. Among those methods in which residual nuclei are detected, there have been many reports of excitation functions.<sup>1</sup> In recent years activation experiments involving the determination of recoil ranges<sup>2-5</sup> or cross-section ratios of isomeric product nuclides ("isomeric ratios") have been emphasized.<sup>6-13</sup> Generally the results are analyzed in terms of the statistical model. Information about nuclear level densities is obtained from excitation functions,<sup>1</sup> while isomeric ratios permit a study of the spin dependence of the level density as well.<sup>6</sup> Recoil ranges help to establish whether a particu-

lar product has the same momentum as that of the incident particle, and whether it was formed by a compound-nuclear reaction.<sup>2-5</sup>

In this paper we emphasize the study of isomeric ratios and recoil ranges for the reactions  $^{41}\text{K}(\alpha, n)^{44}\text{Sc}$ ,  $^{55}\text{Mn}(\alpha, n)^{58}\text{Co}$ ,  $^{93}\text{Nb}(\alpha, n)^{96}\text{Tc}$ ,  $^{93}\text{Nb}(\alpha, 2n)^{95}\text{Tc}$ ,  $^{93}\text{Nb}(\alpha, 3n)^{94}\text{Tc}$ , and  $^{136}\text{Ba}(\alpha, 3n)^{137}\text{Ce}$  in the  $\alpha$ -particle energy range from reaction threshold to 42 MeV. Our primary purpose was to determine isomeric ratios for a group of target and residual nuclei differing widely in mass number and spin. The first experiments involved  $^{41}\text{K}$  and some of those results have been reported previously.<sup>4</sup>

We were also interested in the effect of successive neutron evaporation on the isomeric ratio as in the ( $\alpha, n$ ) and ( $\alpha, 2n$ ) reactions on  $^{93}\text{Nb}$ . At the time this work was begun only a 52-min  $^{94}\text{Tc}$  was known. However, it soon became apparent that a 5-hr isomer of  $^{94}\text{Tc}$  also existed.<sup>14</sup> Another group of investigators discovered it at essentially the same time.<sup>15,16</sup> Thus it became possible to study isomeric ratios in the  $^{93}\text{Nb}(\alpha, 3n)$  reaction as well.

Alpha particles were chosen for the projectiles because they can impact considerable angular momentum, are likely to form compound nuclei, and were available at nearby accelerators.

If isomeric ratios are to be analyzed by a statistical model, one must show that the reaction proceeds predominantly by a compound nuclear mechanism. For this purpose recoil ranges were routinely determined for product nuclei. Excitation functions were also measured, but the accurate determination of absolute cross sections was not emphasized.

\* Supported in part by the U. S. Atomic Energy Commission under contract AT-(30-1)-1930. This is AEC report NYO-1930-41.

† Present address: Department of Chemistry, Faculty of Engineering, Kyushu University, Hakozaki, Fukuoka, Japan.

‡ Present address: Isotopes, Inc., Westwood, New Jersey.

§ Present address: Department of Chemistry, Columbia University, New York, New York.

<sup>1</sup> See, for example, I. Dostrovsky, Z. Fraenkel, and G. Friedlander, *Phys. Rev.* **116**, 683 (1960).

<sup>2</sup> B. G. Harvey, *Ann. Rev. Nucl. Sci.* **10**, 235 (1960).

<sup>3</sup> M. Blann and A. Ewart, *Phys. Rev.* **134**, B783 (1964); J.-P. Hazan and M. Blann, *ibid.* **137**, B1202 (1965).

<sup>4</sup> T. Matsuo and T. T. Sugihara, *Can. J. Chem.* **39**, 697 (1961).

<sup>5</sup> J. M. Alexander and D. H. Sisson, *Phys. Rev.* **128**, 2288 (1962); J. M. Alexander and G. N. Simonoff, *ibid.* **133**, B93 (1964); G. N. Simonoff and J. M. Alexander, *ibid.* **133**, B104 (1964); J. M. Alexander, J. Gilat, and D. H. Sisson, *ibid.* **136**, B1289 (1964); J. Gilat and J. M. Alexander, *ibid.* **136**, B1298 (1964).

<sup>6</sup> R. Vandenbosch and J. R. Huizenga, *Phys. Rev.* **120**, 1313 (1960).

<sup>7</sup> S. Iwata, *J. Phys. Soc. Japan* **17**, 1323 (1962).

<sup>8</sup> C. Bishop, J. R. Huizenga, and J. P. Hummel, *Phys. Rev.* **135**, B401 (1964).

<sup>9</sup> R. L. Kiefer, Lawrence Radiation Laboratory Report No. UCRL-11049, 1963 (unpublished).

<sup>10</sup> A. J. Cox, *Nucl. Phys.* **49**, 577 (1963).

<sup>11</sup> C. Riley and B. Linder, *Phys. Rev.* **134**, B559 (1964).

<sup>12</sup> C. Riley, K. Ueno, and B. Linder, *Phys. Rev.* **135**, B1340 (1964).

<sup>13</sup> R. Vandenbosch, L. Haskin, and J. Norman, *Phys. Rev.* **137**, B1134 (1965).

<sup>14</sup> J. M. Matuszek, Jr. and T. T. Sugihara, *Bull. Am. Phys. Soc.* **8**, 141 (1963); *Nucl. Phys.* **42**, 582 (1963).

<sup>15</sup> S. Monaro, G. B. Vingiani, R. A. Ricci, and R. van Lieshout, *Physica* **28**, 63 (1962).

<sup>16</sup> J. H. Hamilton, K. E. G. Löbner, A. R. Sattler, and R. van Lieshout, *Physica* **30**, 1802 (1964).

The isomeric ratios and their energy dependence are analyzed in detail in the following paper.<sup>17</sup>

## II. EXPERIMENTAL

### A. Targets

Target preparation in the case of <sup>41</sup>K (evaporated as KCl, natural isotopic composition)<sup>4</sup> and <sup>93</sup>Nb (as a self-supporting foil)<sup>14</sup> has been described elsewhere. In the case of <sup>65</sup>Mn, targets were prepared by electro-deposition of the metal onto 0.00015-in. Cu foil from a solution of 10 g MnSO<sub>4</sub>·H<sub>2</sub>O and 15 g (NH<sub>4</sub>)<sub>2</sub>SO<sub>4</sub> in 100 ml H<sub>2</sub>O. A graphite electrode was used as the anode and was separated from the cathode by a porcelain thimble. Crystalline NH<sub>2</sub>OH·HCl was added occasionally to prevent formation of MnO<sub>2</sub>.

Barium targets were prepared by an electrophoretic procedure similar to that described by Bjørnholm.<sup>18</sup> Barium nitrate enriched to 92.9% in <sup>136</sup>Ba was finely ground and suspended in freshly distilled acetone. Electrophoresis of the suspension, which consisted of about 5 mg of salt in 1 ml of acetone, was carried out in a Teflon cell 2.5 cm long, 1 cm wide, and 1 cm high. Aluminum electrodes were located at the ends of the cell, and a 440-V potential was maintained across them. The salt is deposited on the negative electrode.

In all of the experiments, target thicknesses were in the range from 1 to 3 mg/cm<sup>2</sup>, as determined by weighing a piece of known area. Targets were cut to such size as to intercept all of the  $\alpha$ -particle beam in the various accelerators used. No direct determinations of target uniformity were made; however, comparison of different pieces cut from a single prepared target indicated that the thickness did not vary by more than 10% when averaged over areas of the order of 1 cm<sup>2</sup>.

Irradiations were carried out by a conventional stacked-foil technique. For those targets which had a backing material, the latter faced upbeam. High-purity aluminum foil (1.75 mg/cm<sup>2</sup>) was used for recoil catchers immediately downbeam from the target. The catcher area was always larger than that of the target to avoid edge effects. Additional aluminum foil was interspersed between adjacent stacks of target-catcher combinations to degrade the  $\alpha$ -particle energy. Usually the entire collection of targets, catchers, and absorbers was wrapped in aluminum foil before clamping in the target holder.

### B. Irradiations

Irradiations were carried out at the cyclotrons of the Massachusetts Institute of Technology and Brookhaven National Laboratory and at the Yale University Heavy Ion Accelerator. The  $\alpha$ -particle energies incident on the target stack, as indicated by range measurements,

were 31.5±0.2, 40.2±0.2, and 42.0±0.8 MeV, respectively. The energy of  $\alpha$  particles in various targets of the stack was calculated from the range-energy data of Rich and Madey<sup>19</sup> and of Bichsel, Mosley, and Aron.<sup>20</sup> In all experiments in which ranges were determined, a beam collimator was used.

At Brookhaven and Yale the beam intensity was monitored by a Faraday cup. Such an arrangement was not possible at MIT. In order to determine the beam intensity at MIT and to intercalibrate accelerators, a Cu-foil monitor, typically 3.5 mg/cm<sup>2</sup>, was inserted in the target stack for irradiations at all accelerators. The monitoring method<sup>21</sup> depends on measuring the formation cross section of <sup>65</sup>Zn in the reactions <sup>63</sup>Cu( $\alpha$ ,*pn*)<sup>65</sup>Zn and <sup>63</sup>Cu( $\alpha$ ,*2n*)<sup>65</sup>Ga. The latter product nuclide decays with a 15-min half-life to <sup>65</sup>Zn.

### C. Chemical Separations

After irradiation at MIT or Yale, the target stack was usually returned to Clark University before chemical separations were made. In some of the determinations of the <sup>93</sup>Nb( $\alpha$ ,*xn*) cross sections at Yale, radiochemical separation and counting of the short-lived Tc nuclides were done in New Haven. All of the targets irradiated at Brookhaven were processed and counted there.

The methods used to isolate Sc from KCl targets<sup>4</sup> and Tc from Nb targets<sup>14</sup> have been described previously. In the case of Co from a Mn target on Cu foil, the target was dissolved in HNO<sub>3</sub> and carriers were added for Co, Ni, Zn, and Ga. After conversion to an HCl system, Cu was removed as the sulfide. Cobalt was separated by anion exchange with 4*N* HCl after Ni and Mn had been eluted with 6*N* HCl. The sample was converted to K<sub>3</sub>Co(NO<sub>2</sub>)<sub>6</sub>·H<sub>2</sub>O for counting.

In the case of Co recovery from an Al catcher foil, the initial solution was in HCl. Copper carrier in addition to those mentioned for the target was added, and the same general procedure was followed.

In the Ce case, the Ba(NO<sub>3</sub>)<sub>2</sub> target or Al catcher foil was dissolved in HNO<sub>3</sub>, and La and Ce(III) carriers were added. An oxidation-reduction cycle with bromate and H<sub>2</sub>O<sub>2</sub> was carried out twice to ensure exchange between Ce(III) and Ce(IV). Cerium was then precipitated as Ce(IO<sub>3</sub>)<sub>4</sub>, dissolved, and extracted as Ce(IV) into methylisobutyl ketone from 9*M* HNO<sub>3</sub>. The samples were counted as Ce<sub>2</sub>(C<sub>2</sub>O<sub>4</sub>)<sub>3</sub>·9H<sub>2</sub>O.

No chemical separations were necessary to detect <sup>65</sup>Zn in the Cu monitor foils, which were stored for several weeks after irradiation to allow gallium nuclides to decay.

<sup>19</sup> M. Rich and R. Madey, University of California Radiation Laboratory Report No. UCRL-2301, 1954 (unpublished).

<sup>20</sup> H. Bichsel, R. F. Mosley, and W. A. Aron, Phys. Rev. **105**, 1788 (1957).

<sup>21</sup> N. T. Porile and D. L. Morrison, Phys. Rev. **116**, 1193 (1959); F. S. Houck and J. M. Miller, *ibid.* **123**, 231 (1961).

<sup>17</sup> N. D. Dudev and T. T. Sugihara, Phys. Rev. **139**, B896 (1965).

<sup>18</sup> S. Bjørnholm, Nucl. Instr. Methods **5**, 196 (1959).

D. Counting

Pertinent information regarding the decay schemes of the isomers of  $^{44}\text{Sc}$ ,  $^{58}\text{Co}$ ,  $^{23}$  and  $^{24}$   $^{137}\text{Ce}$  is summarized in Table I. The decay schemes of the isomers of  $^{96}\text{Tc}$ ,  $^{95}\text{Tc}$ ,

TABLE I. Gamma rays and branching ratios of  $^{65}\text{Zn}$  and the isomeric pairs  $^{44}\text{Sc}$ ,  $^{58}\text{Co}$ , and  $^{137}\text{Ce}$ .<sup>a</sup>

Nuclide	Half-life	$I\pi$	$E_\gamma$ (MeV)	Branching ratio (%)
$^{44m}\text{Sc}$	57.6 h	$6^+$	0.27 (IT)	100
$^{44g}\text{Sc}$	3.9 h	$2^+$	1.16	100
$^{58m}\text{Co}$	9.2 h	$5^+$	0.025 (IT)	100
$^{58g}\text{Co}$	71 day	$2^+$	0.511 ( $\beta^+$ )	15
			0.799	99
$^{65}\text{Zn}$	245 day	$5^-$	0.511 ( $\beta^+$ )	1.7
			1.114	49
$^{137m}\text{Ce}$	34.5 h	$1\frac{1}{2}^+$	0.255 (IT)	100
$^{137g}\text{Ce}$	8.7 h	$3^-$	0.445	3
			0.010	100

<sup>a</sup> From Ref. 22 for  $^{44}\text{Sc}$ , Ref. 23 for  $^{58}\text{Co}$  and  $^{65}\text{Zn}$ , and Ref. 24 for  $^{137}\text{Ce}$ .

and  $^{94}\text{Tc}$  are considerably more complex; these are shown in Figs. 1, 2, and 3. In general, detection was based on  $\gamma$  rays or x rays. For the isomeric pairs of  $^{44}\text{Sc}$ ,  $^{58}\text{Co}$ ,  $^{96}\text{Tc}$ , and  $^{137}\text{Ce}$ , the metastable state decays essentially only to the ground state. In principle, the activity of the former can be deduced from that of the latter; this method has the advantage that the detection efficiency is not involved in calculating the isomeric ratio. For practical reasons, however, which are specified below, the isomers of  $^{96}\text{Tc}$  and  $^{137}\text{Ce}$  were not counted in this fashion.

The choices of detector and auxiliary electronics were based chiefly on equipment available at the laboratory

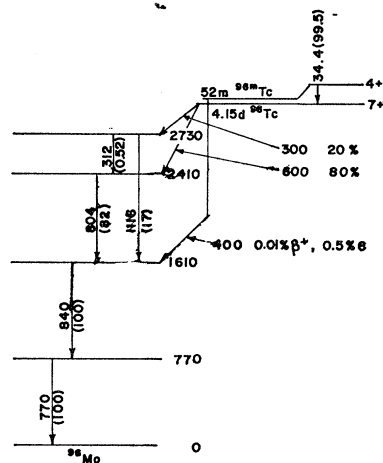


FIG. 1. Decay scheme of  $^{96m}\text{Tc}$  and  $^{96g}\text{Tc}$ , from Ref. 23. All energies are in keV. Quantities in parentheses are percentages of decay events which lead to a particular transition.

<sup>22</sup> J. D. McCullen and J. J. Kraushaar, Phys. Rev. **122**, 555 (1961); D. L. Harris and J. D. McCullen, Phys. Rev. **132**, 310 (1963).

<sup>23</sup> Nuclear Data Sheets, compiled by K. Way et al. (Printing and Publishing Office, National Academy of Sciences-National Research Council, Washington 25, D. C.), NRC 59-2-23, 59-4-60, 60-5-12, 60-5-120, 60-6-33, and 61-2-137.

<sup>24</sup> A. R. Brosi and B. H. Ketelle, Phys. Rev. **100**, 169 (1955); **103**, 917 (1956).

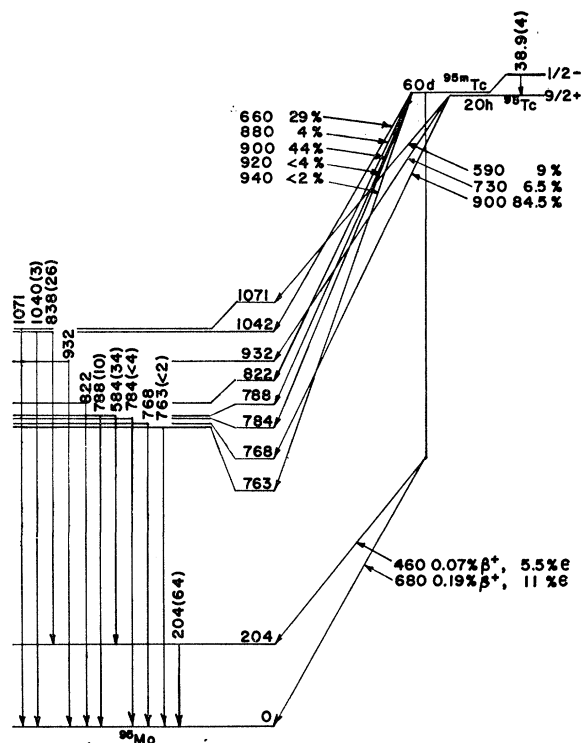


FIG. 2. Decay scheme of  $^{95m}\text{Tc}$  and  $^{95g}\text{Tc}$ , from Ref. 23. All energies are in keV. Quantities in parentheses are percentages of decay events of  $^{95m}\text{Tc}$  which lead to a particular transition.

during the several years devoted to these experiments. The most recent experiments are those in which the target mass is largest. The efficiencies of the various scintillation detectors were determined as a function of  $\gamma$ -ray energy by the use of standards obtained from commercial sources and the National Bureau of Standards. Efficiencies are known to about 10%.

In the case of the Tc nuclides, all decay curves were resolved with the help of the least-squares program FRANTIC<sup>25</sup> because of the many half-lives involved in the gross decay curve. No such treatment was necessary for  $^{44}\text{Sc}$ ,  $^{58}\text{Co}$ , or  $^{137}\text{Ce}$  which were analyzed by the usual graphical or analytical methods.

1.  $^{44m}\text{Sc}$  and  $^{44g}\text{Sc}$

The cross sections of  $^{44m}\text{Sc}$  and  $^{44g}\text{Sc}$  were based on following the decay of the 1.16-MeV  $\gamma$  ray in the ground-state nuclide. Details have been given previously.<sup>4</sup>

2.  $^{58m}\text{Co}$  and  $^{58g}\text{Co}$

Cross sections for the  $^{58}\text{Co}$  isomers were determined by resolving the decay curve of the 799-keV  $\gamma$  ray. Counting was done on either a 3.7-cm $\times$ 5.1-cm or a 7.6-cm $\times$ 7.6-cm NaI(Tl) crystal coupled either with a

<sup>25</sup> P. C. Rogers, Massachusetts Institute of Technology Report No. NYO-2303, 1962 (unpublished).

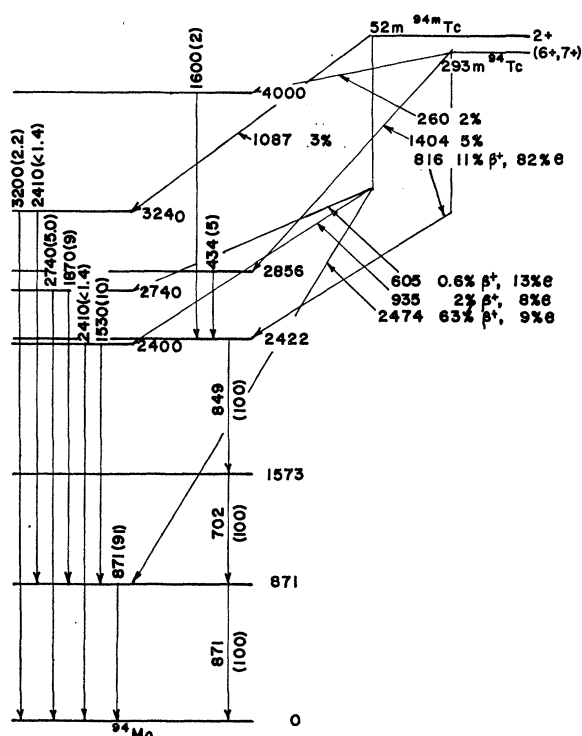


FIG. 3. Decay scheme of  $^{94m}\text{Tc}$  and  $^{94g}\text{Tc}$ , from Ref. 16. All energies are in keV. Gamma rays in the decay of  $^{94m}\text{Tc}$  are grouped on the left and those of  $^{94g}\text{Tc}$  on the right. Quantities in parentheses are percentages of decay events which lead to a particular transition.

single-channel analyzer set to include the energy region 700–900 keV or in some cases with a multichannel analyzer. Above the threshold for the  $^{55}\text{Mn}(\alpha,3n)$  reaction, interference from the radiations of 77-day  $^{56}\text{Co}$  became troublesome, particularly a 845-keV  $\gamma$  ray of high intensity.<sup>23</sup> Up to  $\approx 30$  MeV it was possible to correct for the contribution of  $^{56}\text{Co}$  to the observed activity in the 800-keV region.

The correction was made in the following manner. A sample of  $^{56}\text{Co}$ , free from  $^{58g}\text{Co}$ , was prepared by the  $^{56}\text{Fe}(p,n)$  reaction. The decay of  $^{56}\text{Co}$  includes also a 1260-keV  $\gamma$  ray. There is no  $\gamma$  ray of comparable energy in the decay of  $^{58m}\text{Co}$ . By empirically establishing for a particular experimental counting arrangement the relative intensities in the 1260- and 800-keV regions in  $^{56}\text{Co}$ , we could correct the observed  $\gamma$ -ray spectra of mixed  $^{58g}\text{Co}$  and  $^{56}\text{Co}$  for the contribution of the latter. This method was not considered to be reliable when the correction was more than 50%.

### 3. $^{96m}\text{Tc}$ and $^{96g}\text{Tc}$

Cross sections for these nuclides were deduced from resolving the decay curve of  $K$  x rays. Both the isomeric transition in  $^{96m}\text{Tc}$  and the electron-capture decay of  $^{96g}\text{Tc}$  lead to  $K$  x rays. While it should be possible to determine both cross sections by following the decay of

one of the  $\gamma$  rays in the decay of  $^{96g}\text{Tc}$ , the large difference in the half-lives of the two nuclides and the fact that the ground-state yield was usually much larger than the metastable-state yield meant that observed decay curves did not show an appreciable growth which could be resolved with precision to give a 52-min component. Hence it was necessary to observe radiations from  $^{96m}\text{Tc}$  directly.

The  $K$  x rays were detected by a NaI(Tl) crystal of thickness 6 mm and measuring 2 cm by 2 cm in area. The 18-keV  $K$  x rays of Tc and Mo had a resolution (full width at half-maximum) of  $\approx 50\%$ . The crystal was usually operated only with a base-line discriminator set at 8 keV. The crystal had a very limited sensitivity to electromagnetic radiation of energy above  $\approx 90$  keV. Operating with an integral bias, we found 86% of the total integral activity above 8 keV to be under the  $K$  x-ray photopeak for a sample of  $^{96g}\text{Tc}$ .

This detection method runs into difficulty above the  $^{93}\text{Nb}(\alpha,3n)$  threshold, since one of the isomers of  $^{94}\text{Tc}$  has a 52-min half-life and emits x rays in its decay.<sup>14</sup> We report  $^{96m}\text{Tc}$  data only up to a bombarding energy of 27 MeV.

The ratio of conversion coefficients  $\alpha_K/\alpha_L$  for the isomeric transition was estimated to be 0.86 by extrapolation of the calculated values of Sliv and Band.<sup>26</sup> Conversion in  $M$  and higher shells was disregarded. The  $K$  fluorescence yield<sup>27</sup> in Tc and Mo was taken to be 0.75. In the decay of the ground state, the ratio of  $L$  capture to  $K$  capture<sup>28</sup> (assumed to be the same for both electron-capture branches) was calculated to be 0.116. The  $(M+N)/L$  capture ratio<sup>28</sup> was taken to be 0.165.

### 4. $^{95m}\text{Tc}$ and $^{95g}\text{Tc}$

To a first approximation the metastable nuclide does not decay to the ground state; hence each must be detected separately. We have used integral-bias counting on a well scintillation crystal [NaI(Tl), 3.8 cm diam by 5 cm high] operated with a discriminator set at 75 keV. According to the decay scheme,<sup>23</sup> there are 1.45  $\gamma$  rays of energy above 75 keV per disintegration of  $^{95m}\text{Tc}$ , if it is assumed that 5.4% of the 204-keV  $\gamma$  rays are converted. The weighted-average efficiency under our conditions for these  $\gamma$  rays was interpolated to be 0.431. In the ground-state decay there is one  $\gamma$  ray per disintegration and the weighted-average efficiency on the well counter was 0.355.

The half-lives of the  $^{95}\text{Tc}$  pair are sufficiently different from those of the  $^{94}\text{Tc}$  and  $^{96}\text{Tc}$  pairs that the  $(\alpha,2n)$  products could be determined essentially without interference by resolution of decay curves.

<sup>26</sup> L. Sliv and I. Band, *Coefficients of Internal Conversion of Gamma Rays* (Academy of Sciences of the USSR, Moscow, 1956).

<sup>27</sup> H. L. Hagerdorn and A. H. Wapstra, *Nucl. Phys.* **15**, 146 (1960).

<sup>28</sup> H. Brysk and M. E. Rose, Oak Ridge National Laboratory Report No. ORNL-1830, 1955 (unpublished).

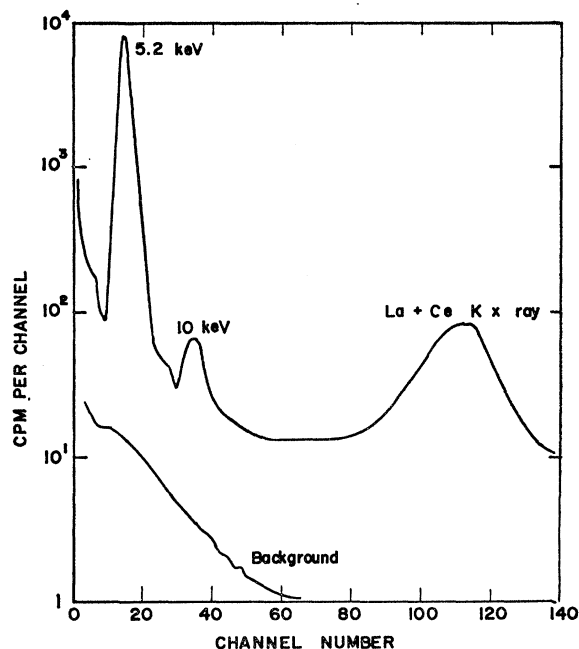


Fig. 4. Spectrum of pulses in proportional counter from source of  $^{137m}\text{Ce}$ - $^{137g}\text{Ce}$  (upper curve) and from background of unshielded counter (lower curve).

#### 5. $^{94m}\text{Tc}$ and $^{94g}\text{Tc}$

Details of the counting method have been given elsewhere.<sup>14</sup> Briefly, the cross section of 52-min  $^{94m}\text{Tc}$  was obtained by resolving the decay curve of 871-keV  $\gamma$  rays, as measured on a 10-cm $\times$ 10-cm NaI(Tl) crystal coupled with a multichannel analyzer. The activity of 293-min  $^{94g}\text{Tc}$  was determined from analysis of the decay of the  $\gamma$  rays of 702, 849, and 871 keV. Calculated cross sections are based on the decay scheme of Ref. 16.

#### 6. $^{137m}\text{Ce}$ and $^{137g}\text{Ce}$

In principle these two nuclides could be determined by a parent-daughter analysis of the 445-keV transition in the decay of the ground state. However, its abundance is low ( $\approx 3\%$ ); it is simpler and more precise to follow the decay of the two species by detection of  $L$  x rays. This was done on a cylindrical proportional counter,<sup>29</sup> 46 cm long and 5 cm diam, made of a graphite-impregnated phenolic-resin tube with an anode of stainless steel wire. A Mylar foil was taped over a window opening (5 cm $\times$ 5 cm) cut in the wall. The counter was operated as a flow counter at  $\approx 1200$  V with P-10 gas. The signal was fed to a modified Los Alamos model-100 preamplifier and then to the internal amplifier of a Nuclear Data multichannel analyzer.

Typical x-ray and background spectra are shown in Fig. 4. The 5.2-keV peak consists of  $L$  x rays of  $^{137}\text{La}$

<sup>29</sup> C. Gatrousis, R. Heinrich, and C. E. Crouthamel, in *Progress in Nuclear Energy*, edited by C. Crouthamel (Pergamon Press, New York, 1961), Vol. 2, Chap. I.

and  $^{137}\text{Ce}$ , while the 10-keV peak corresponds to the 10-keV  $\gamma$  ray in the decay of  $^{137}\text{Ce}$ . The background rate is with the counter unshielded. The resolution for 5-keV radiation is  $\approx 20\%$ .

Samples were counted through a beryllium absorber, 30 mg/cm<sup>2</sup> thick, which was sufficient to stop Auger electrons and reduce markedly the efficiency for counting  $\beta$  particles. Corrections for self-absorption of  $L$  x rays in counting samples were made according to an empirically determined correction curve.

The details of the method by which the decay curve of 5-keV radiation was analyzed and converted to cross sections for  $^{137m}\text{Ce}$  and  $^{137g}\text{Ce}$  are given in an Appendix.

#### 7. $^{65}\text{Zn}$

The total  $^{65}\text{Zn}$  activity produced in the monitor reaction was determined by scintillation counting of its 1.114-MeV  $\gamma$  ray, on either the well crystal or a 10-cm $\times$ 10-cm solid crystal.

### III. CALCULATIONS OF EXPERIMENTAL DATA AND RESULTS

Observed activities were converted to cross sections by the usual equations. In some cases in which the irradiation time was appreciable compared to the half-life of a nuclide detected, two additional factors had to

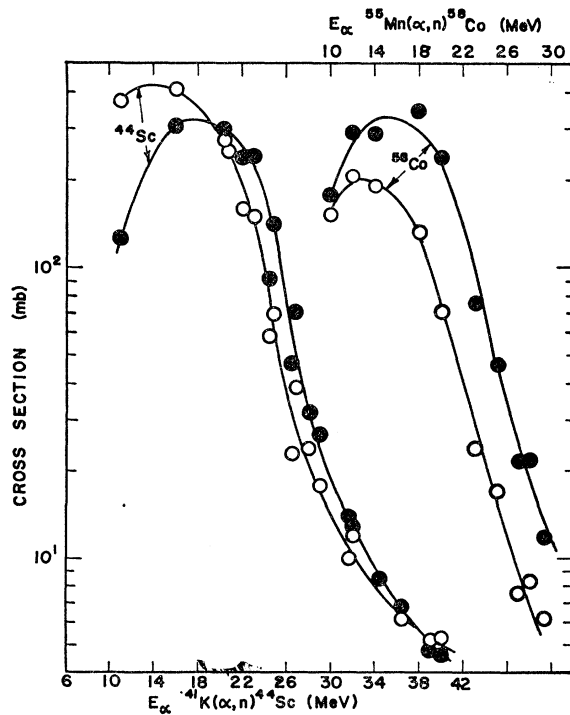


Fig. 5. Excitation functions for the reactions  $^{41}\text{K}(\alpha, n)$  and  $^{55}\text{Mn}(\alpha, n)$ . Open circles denote the ground-state nuclide and filled circles the metastable nuclide. Bombarding energy is in the laboratory system. The lower energy scale is for the  $^{41}\text{K}(\alpha, n)$  reaction and the upper scale for the  $^{55}\text{Mn}(\alpha, n)$  reaction.

TABLE II. Isomeric ratio  $\sigma(\text{high spin})/\sigma(\text{low spin})$  of product nuclei in reactions  $^{41}\text{K}(\alpha, n)$ ,  $^{55}\text{Mn}(\alpha, n)$ ,  $^{93}\text{Nb}(\alpha, xn)$ , and  $^{136}\text{Ba}(\alpha, 3n)$ . Errors are estimated from counting statistics and reproducibility of determinations.

$E_\alpha^*$ (MeV)	$^{44}\text{Sc}$	$^{58}\text{Co}$	$^{96}\text{Tc}$	$^{98}\text{Tc}$	$^{94}\text{Tc}$	$^{137}\text{Ce}$
6.0	0.30±0.03					
10.5			0.18±0.12			
11.0	0.34±0.04		0.41±0.04			
12.0		1.1±0.1	0.33±0.04			
12.5			0.34±0.03			
13.0			0.29±0.02			
14.0		1.4±0.1	0.34±0.03			
14.5			0.50±0.07			
15.0			0.47±0.04			
15.5			0.59±0.05			
16.0	0.75±0.08	1.5±0.1	0.63±0.05			
18.0		2.6±0.1	1.02±0.08			
18.5				5.9±0.3		
19.0	1.1 ±0.1	3.3±0.2	1.23±0.10	5.9±0.3		
19.5	1.2 ±0.1		1.50±0.10			
20.0		3.4±0.2				
22.0	1.55±0.07			6.9±0.4		
22.5				7.0±0.5		
23.0	1.6 ±0.1	3.2±0.2	1.73±0.10	7.2±0.5		
23.5			1.31±0.21			
24.0				7.2±0.5		
24.5	1.6 ±0.1					
25.0	2.0 ±0.1	2.8±0.2				
25.5				8.1±0.6		
26.0			0.62±0.10	7.8±0.6		
26.5	1.9 ±0.2			8.7±0.6		
27.0		2.5±0.3		9.0±0.6	1.4±0.2	
28.0	1.3 ±0.1	2.6±0.2	0.46±0.14	9.6±0.5		3.5±0.3
29.0	1.5 ±0.1				2.4±0.2	
29.5		1.9±0.2		10.6±0.6		3.3±0.3
30.0					2.5±0.5	
30.5				11.0±0.6		
31.5	1.3 ±0.1					4.8±0.4
32.0	1.12±0.06					
33.0				11.8±0.6	4.3±0.5	5.6±0.8
33.5				10.7±0.7		
34.0				11.7±0.6	3.2±0.5	6.1±0.5
34.5	1.0 ±0.1			10.1±0.6		5.5±0.4
35.0				11.4±1.0		
35.5				10.1±0.4		
36.0					5.3±0.7	7.8±0.6
36.5				9.0±0.6		
37.0						8.9±0.8
38.0				8.2±0.6	5.0±0.8	9.9±1.1
38.5				7.8±0.4		
39.0	0.94±0.06				5.9±0.8	9.0±0.6
39.5					5.8±1.1	
40.0	0.9 ±0.1			6.1±0.4		11.3±1.9
42.0				4.9±0.4	6.3±0.7	

\* Median laboratory energy of  $\alpha$  particle, rounded off to nearest 0.5 MeV.

be considered. Proper account was taken for the formation of daughter activity from the decay of its parent during the irradiation. Secondly, fluctuations in the beam intensity were taken into account as necessary. For calculation purposes the irradiation time was broken up into intervals in which the beam intensity was fairly uniform.

In general, the targets were thin enough that an appreciable fraction of products formed recoiled into the catchers. For cross-section calculations, the activity in the catcher (corrected for chemical yield) was added to that left in the target.

Since the chief purpose of these experiments was to determine isomeric ratios rather than absolute cross

sections, the procedures were designed primarily for precision in the ratio and less attention was paid to the factors affecting absolute cross sections. The results are reported in Table II, which lists isomeric ratios for the several reactions. Some of the data are shown graphically in the following paper.<sup>17</sup> Bombarding energies have been rounded off to the nearest 0.5 MeV. The dispersion in the incident beam plus that introduced by straggling in absorbers makes a more precise statement of the  $\alpha$ -particle energy meaningless. Excitation functions are given in Figs. 5-7.

In a thick-target, thick-catcher experiment, the fraction of the activity produced which recoils out of the target is a measure of the average range in the

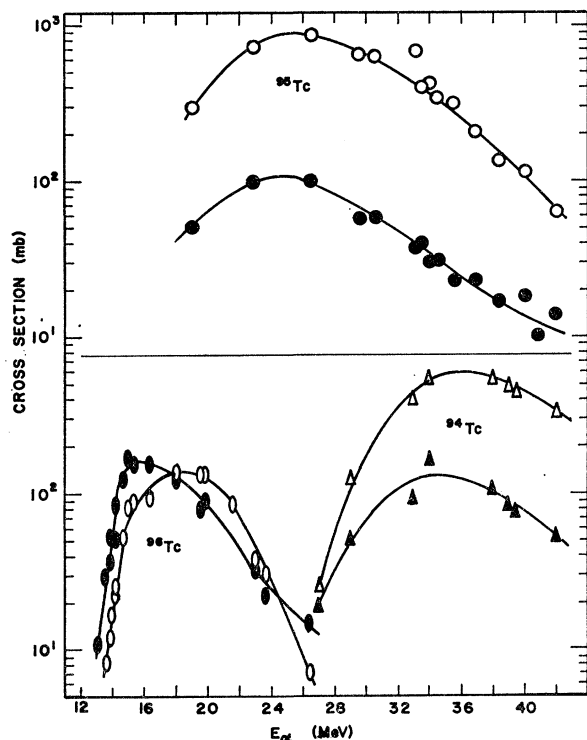


FIG. 6. Excitation functions for the  $(\alpha, n)$ ,  $(\alpha, 2n)$ , and  $(\alpha, 3n)$  reactions of  $^{93}\text{Nb}$ . In each case the open symbol refers to the ground-state nuclide and the filled symbol to the metastable nuclide. Bombarding energy is in the laboratory system.

target material, projected in the beam direction, according to<sup>30</sup>

$$R_p = WF, \quad (1)$$

where  $W$  is the target thickness and  $F$  is the fraction of the activity produced which is found in the forward catcher. The average projected range  $R_p$  is converted to the average range  $R$  by<sup>31</sup>

$$R \approx R_p(1 + \mu/3), \quad (2)$$

where  $\mu$  is the ratio of masses of stopping atoms to recoiling atoms.

Experimental values of  $R$  for  $^{44}\text{Sc}$  in KCl and for  $^{58}\text{Co}$  in Mn are listed in Table III. Similar range data for  $^{94}\text{Tc}$ ,  $^{95}\text{Tc}$ , and  $^{96}\text{Tc}$  in Nb and  $^{137}\text{Ce}$  in  $\text{Ba}(\text{NO}_3)_2$  are given in Table IV.

If the  $(\alpha, xn)$  reaction products studied here have received the full momentum of the incident ion, the recoil energy of a product nuclide is given by

$$E_p = E_\alpha M_\alpha M_p (M_t + M_\alpha)^{-2}, \quad (3)$$

where  $E$  and  $M$  refer to kinetic energy and mass, and the subscripts  $p$ ,  $\alpha$ , and  $t$  denote product,  $\alpha$  particle, and

<sup>30</sup> L. Winsberg and J. M. Alexander, Phys. Rev. **121**, 518 (1959).

<sup>31</sup> J. Lindhard and M. Scharff, Phys. Rev. **124**, 128 (1961).

TABLE III. Experimental average ranges  $R$  of  $^{44m}\text{Sc}$  and  $^{44g}\text{Sc}$  in KCl as produced in the  $^{41}\text{K}(\alpha, n)$  reaction and of  $^{58m}\text{Co}$  and  $^{58g}\text{Co}$  in Mn as produced in the  $^{55}\text{Mn}(\alpha, n)$  reaction. The last two columns are calculated LSS ranges  $R_0$  for  $^{44}\text{Sc}$  (both isomers) in KCl and  $^{58}\text{Co}$  (both isomers) in Mn. The calculation assumes complete momentum transfer and neglects neutron evaporation.

$E_{\alpha^a}$ (MeV)	Experimental ranges ( $\mu\text{g}/\text{cm}^2$ of target)				Calculated ranges in target	
	$^{44m}\text{Sc}$	$^{44g}\text{Sc}$	$^{58m}\text{Co}$	$^{58g}\text{Co}$	KCl	Mn
19.0			$647 \pm 26$	$651 \pm 26$		349
23.0	$522 \pm 25$	$529 \pm 25$	$707 \pm 30$	$617 \pm 30$	500	402
27.0			$791 \pm 35$	$636 \pm 35$		465
32.0	$507 \pm 25$	$462 \pm 25$			640	
39.0	$633 \pm 30$	$550 \pm 30$			740	

<sup>a</sup> Median laboratory energy of  $\alpha$  particle, rounded off to nearest 0.5 Mev.

TABLE IV. Experimental average ranges  $R$  of  $^{96}\text{Tc}$ ,  $^{95}\text{Tc}$ , and  $^{94}\text{Tc}$  in Nb as produced in the  $^{93}\text{Nb}(\alpha, xn)$  reactions and of  $^{137}\text{Ce}$  in  $\text{Ba}(\text{NO}_3)_2$  as produced in  $^{136}\text{Ba}(\alpha, 3n)$  reaction. The last two columns are calculated LSS ranges  $R_0$  for Tc nuclides in Nb and for  $^{137}\text{Ce}$  in  $\text{Ba}(\text{NO}_3)_2$ . The calculation assumes complete momentum transfer and neglects neutron evaporation.

$E_{\alpha^a}$ (MeV)	Experimental ranges ( $\mu\text{g}/\text{cm}^2$ of target)				Calculated ranges in target ( $\mu\text{g}/\text{cm}^2$ )	
	$^{96}\text{Tc}$	$^{95}\text{Tc}$	$^{94}\text{Tc}$	$^{137}\text{Ce}$	Nb	$\text{Ba}(\text{NO}_3)_2$
15.0	$120 \pm 20$				130	
16.0	$103 \pm 20$				142	
18.5	$174 \pm 24$	$176 \pm 26$			160	
19.0	$143 \pm 20$	$135 \pm 20$			163	
19.5	$170 \pm 27$				170	
23.0	$186 \pm 28$	$190 \pm 28$			195	
27.0	$181 \pm 27$	$224 \pm 33$			226	
28.0				$81 \pm 16$		83
28.5				$60 \pm 13$	250	88
30.5	$171 \pm 25$	$278 \pm 41$			257	
31.5	$157 \pm 22$	$210 \pm 31$				95
33.0				$112 \pm 22$		99
33.5	$156 \pm 19$	$262 \pm 40$	$253 \pm 39$		129 $\pm$ 26	277
34.5	$181 \pm 27$	$291 \pm 43$	$277 \pm 42$	$117 \pm 20$		286
35.5	$196 \pm 30$	$276 \pm 41$	$334 \pm 52$	$148 \pm 28$		294
36.0						109
36.5	$219 \pm 33$	$252 \pm 50$	$288 \pm 45$			300
38.0				$146 \pm 29$		114
38.5	$163 \pm 25$	$240 \pm 36$				315
40.0		$273 \pm 42$	$331 \pm 51$			325
40.5	$198 \pm 33$					330
42.0	$158 \pm 24$	$241 \pm 50$	$230 \pm 46$			338

<sup>a</sup> Median laboratory energy of  $\alpha$  particle, rounded off to nearest 0.5 Mev.

target nucleus, respectively. The effect of neutron evaporation on  $E_p$  is discussed in Sec. IV.

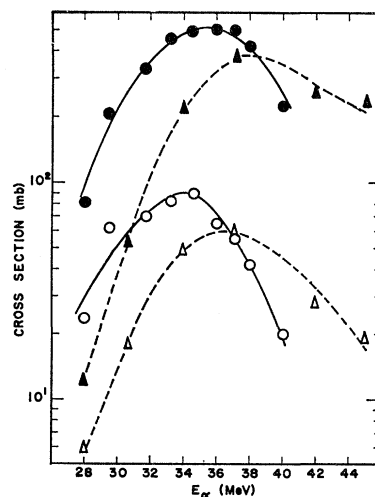


FIG. 7. Excitation functions for  $^{137m}\text{Ce}$  (filled symbols) and  $^{137g}\text{Ce}$  (open symbols) in the reaction  $^{136}\text{Ba}(\alpha, 3n)$ . The circles are the results from this work and the triangles are data taken from Ref. 9. Bombarding energy is in the laboratory system.

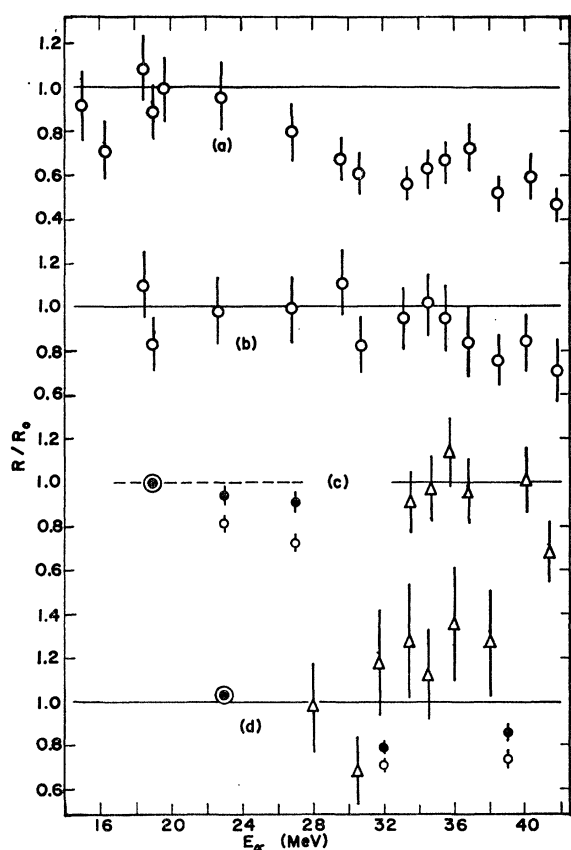


FIG. 8. Average recoil ranges  $R$  of product nuclides in units of the LSS range  $R_0$  as a function of bombarding energy in the laboratory system. The experimental points in (a) and (b) are for  $^{96}\text{Tc}$  and  $^{95}\text{Tc}$ , respectively. In (c) and (d) the triangles are experimental ranges for  $^{94}\text{Tc}$  and  $^{137}\text{Ce}$ , respectively. The circles in (c) and (d) refer to  $^{58}\text{Co}$  and  $^{44}\text{Sc}$ , respectively. Open circles denote the ground-state nuclide and filled circles the metastable nuclide. The solid horizontal lines at  $R/R_0=1$  represent the ranges expected if the LSS range-energy relationship is correct and if the product nuclide has a recoil energy given by Eq. (3). The dashed horizontal line in (c) results from normalization at  $E_\alpha=19$  MeV (see text for details).

Lindhard, Scharff, and Schiøtt<sup>32</sup> (referred to hereafter as LSS) have recently derived a "universal" range-energy relationship which appears in general to account for experimental data very well.<sup>3</sup> We have calculated the LSS range  $R_0$  for each product nuclide at each bombarding energy for which recoil data were available. In using the relationship, we assume that the kinetic energy of the product nuclide is that given by Eq. (3). Some stopping materials such as KCl and  $\text{Ba}(\text{NO}_3)_2$  contain more than one element. In these cases  $R_0^{(i)}$  was calculated for each element  $i$  and  $R_0$  for the compound was taken as

$$1/R_0 = \sum_i (w_i/R_0^{(i)}),$$

where  $w_i$  is the fraction by weight of element  $i$  in the compound.

<sup>32</sup> J. Lindhard, M. Scharff, and H. E. Schiøtt, Kgl. Danske Videnskab. Selskab, Mat. Fys. Medd. 33, No. 4 (1963).

In Fig. 8 experimental ranges  $R$  are shown in units of  $R_0$  (except in the case of  $^{58}\text{Co}$  which is discussed separately). If the LSS relationship is correct, deviations from the horizontal lines represent the extent to which experimental recoil energies differ from that calculated from Eq. (3).

Observed ranges of the  $^{58}\text{Co}$  isomers were consistently larger than that expected from the LSS relationship for Mn. The Mn targets had an oxide layer of indeterminate thickness on the surface; a correction for this would make experimental ranges still larger. We have no explanation for the discrepancy. For the purposes of Fig. 8 we have normalized the observed range to the LSS range at 19 MeV and have used the same normalization factor (1.87) to correct observed ranges at 23 and 27 MeV.

In some cases the recoil ranges of an isomeric pair are sufficiently different from each other that they can be separately analyzed. Such an analysis has been given previously<sup>4</sup> for the  $^{44}\text{Sc}$  pair in the  $^{41}\text{K}(\alpha, n)$  reaction, where differential ranges were also available, to extract information about the relative contribution of a reaction mechanism in which momentum transfer was incomplete. In general, however, the difference in range between an isomeric pair is smaller than the errors of the measurement, particularly for the heavier target nuclei, for which case  $E_p$  is small and the fraction  $F$  is correspondingly small. For the heavier nuclei the experimental points represent the average value for both isomers. In the case of  $^{96}\text{Tc}$  for  $E_\alpha > 26$  MeV, the fraction recoiling out was measured only for 4.1-day  $^{96g}\text{Tc}$  at a time after irradiation when the decay of 52-min  $^{96m}\text{Tc}$  to the ground state was essentially complete.

We estimate from counting statistics and reproducibility of replicate determinations that in general the isomeric ratios reported have random errors of less than 10%. Systematic errors are possible if the decay schemes used are incorrect. Errors affecting the shape of the excitation functions are estimated to be less than 25%; their absolute magnitudes may have appreciable systematic errors, as in the case of  $^{137}\text{Ce}$  whose cross section depends critically on the value chosen for the  $L$ -shell fluorescence yield. In the case of recoil ranges, estimated errors run from 5% for light nuclei such as  $^{44}\text{Sc}$  to 20% for  $^{137}\text{Ce}$ . Here chemical-yield determinations and target uniformity contribute to the over-all error.

#### IV. DISCUSSION

A detailed analysis of the magnitude and energy dependence of isomeric ratios is given in the following paper.<sup>17</sup> Only a qualitative discussion is presented here. The three  $(\alpha, n)$  and the  $(\alpha, 2n)$  ratios all go through a maximum. The rising portion is attributed to the increasing average spin of the compound nucleus as the  $\alpha$ -particle energy increases. The decreasing region in the  $(\alpha, n)$  reactions probably indicates that a process



involving low momentum transfer is contributing. In the  $(\alpha, 2n)$  case, however, the evidence from range measurements suggests that such a contribution is probably not very large. This point is discussed further below and in the following paper.

The dependence of recoil range on  $\alpha$ -particle energy is a useful tool in this sort of analysis. In the  $^{41}\text{K}(\alpha, n)^{44}\text{Sc}$  reaction at 40 MeV,  $\approx 46\%$  of  $^{44}\text{Sc}$  was estimated<sup>4</sup> to be formed in a non-compound-nuclear reaction, and  $\approx 30\%$  in the case of  $^{44m}\text{Sc}$ . For the other product nuclides (except  $^{58}\text{Co}$ ) the ranges of isomeric pairs were not sufficiently different that they could be analyzed in the same way. In the case of  $^{58}\text{Co}$  the indications are that the low-spin ground state has a significantly smaller range than that of the high-spin  $^{58m}\text{Co}$  for  $E_\alpha \gtrsim 23$  MeV. Detailed analysis has not been made, however, because of the difficulties mentioned earlier.

Blann and co-workers,<sup>3</sup> who have made extensive use of recoil ranges to study nuclear reactions, have discussed in detail the sensitivity of range measurements to reaction mechanisms. Since range is not proportional to momentum, in the region of recoil energies of interest to us, neutron evaporation will affect the average range. In general, the range of the product nuclide is a few percent higher than that of the compound nucleus on reasonable assumptions<sup>3</sup> regarding the kinetic energy and angular distributions of evaporated neutrons. Since a correction for evaporation has not been made, observed ranges  $R$  should be slightly greater than  $R_0$  if the reaction is compound nuclear.

In all of the  $(\alpha, n)$  reactions, the measured range is significantly less than  $R_0$  when  $E_\alpha$  is 5 MeV or more above the energy at which the excitation function goes through a maximum. The  $^{93}\text{Nb}(\alpha, 2n)$ ,  $^{93}\text{Nb}(\alpha, 3n)$ , and  $^{136}\text{Ba}(\alpha, 3n)$  ranges are generally consistent with a process in which there is complete momentum transfer at all of the observed energies, though there is some scatter in the experimental data.

The  $^{98}\text{Tc}$  ranges in the energy region above 35 MeV might be considered to be systematically too small for a compound-nuclear reaction, but experimental errors are sufficiently large that such a conclusion is not warranted. It seems unlikely, however, that there is a large contribution of a mechanism in which momentum transfer is small. Yet above 35 MeV, the isomeric ratio decreases monotonically and rapidly with bombarding energy. Probably the decrease in the ratio should not be ascribed entirely to a direct interaction.

The excitation functions qualitatively exhibit the shape expected from the discussion above. All of the  $(\alpha, n)$  excitation functions have a high-energy tail. There is some evidence in the  $^{93}\text{Nb}(\alpha, 2n)^{95m}\text{Tc}$  excitation function for such a tail also. The  $(\alpha, 3n)$  excitation functions show the typical compound-nuclear shapes.<sup>1</sup> The maxima of excitation functions of an isomeric pair are in general displaced; that of the high-spin state occurs at a higher energy. The displacement is particularly apparent in the  $(\alpha, n)$  reactions.

Some of these experiments have also been done by others. Recently, Riley *et al.*<sup>12</sup> reported cross sections and isomeric ratios for the reaction  $^{41}\text{K}(\alpha, n)^{44}\text{Sc}$  for bombarding energies between 8 and 19 MeV. The cross sections determined in this work are in general larger than those of Riley *et al.* in the energy region in which the two sets of data overlap. The isomeric ratios are in agreement at 11 MeV; at 16 and 19 MeV, however, our results are  $\approx 35\%$  lower. The differences can probably be ascribed to differences in beam intensities of the accelerator used (tandem Van de Graaff versus cyclotron) and in counting methods. Our work has emphasized accuracy in isomeric ratios rather than in absolute cross sections; the counting method which we have used does not depend critically on the decayscheme of  $^{44}\text{Sc}$  and detection efficiency is not involved in calculating isomeric ratios. Because of the low intensity of  $\alpha$  particles from a Van de Graaff generator, Riley *et al.* were forced to detect  $^{44m}\text{Sc}$  and  $^{44g}\text{Sc}$  separately. Their calculated isomeric ratio depends on knowing accurately the conversion coefficient of the isomeric transition and the detection efficiencies of both nuclides.

Iwata<sup>7</sup> has also measured the isomeric ratio in the reaction  $^{55}\text{Mn}(\alpha, n)^{58}\text{Co}$ . His results, using the same counting method, are about 25% higher than those reported here, but the energy dependence of the two sets of isomeric ratios is the same. Iwata does not report absolute cross sections.

Kiefer<sup>9</sup> has recently reported results for the  $^{136}\text{Ba}(\alpha, 3n)^{137}\text{Ce}$  reaction (see Fig. 7). He detected the  $^{137}\text{Ce}$  isomers by counting the 445-keV ground-state  $\gamma$  ray which has a 3% branching ratio. His isomeric ratios are consistently lower than those of this work by about 30%. Both sets of data show the same monotonic increase in the ratio with increasing  $E_\alpha$ . In the case of the excitation functions, a shift in the energy axis ( $\approx 3$  MeV) is necessary in order to obtain reasonable agreement. Such an energy shift would also make the agreement between the isomeric-ratio curves very much better. It is difficult to imagine, however, that the Brookhaven cyclotron, where our work was done, and the University of California 60-in cyclotron would disagree in energy calibration by such a large amount.

#### ACKNOWLEDGMENTS

We are greatly indebted to Dr. P. T. Demos and E. White of the Massachusetts Institute of Technology, Professor R. Beringer and Dr. I. Preiss of Yale University, and Dr. R. W. Dodson, Dr. C. P. Baker, and Dr. J. Hudis of the Brookhaven National Laboratory for their cooperation in making available to us the accelerators, radiochemical facilities, and detectors used in the experiments described here. The cooperation of Dr. P. C. Rogers and the operating staff of the Compton Computation Center of Massachusetts Institute of Technology is gratefully acknowledged.

## APPENDIX

The decay curve of the 5-keV peak in the decay of  $^{137m}\text{Ce}$  and  $^{137g}\text{Ce}$  was analyzed in the following manner. The disintegration rates  $A$  of the metastable state  $m$  or ground state  $g$  as a function of time  $t$  are

$$A_m = A_m^0 \exp(-\lambda_m t) \quad (\text{A1})$$

and

$$A_g = q A_m^0 [\exp(-\lambda_m t) - \exp(-\lambda_g t)] + A_g^0 \exp(-\lambda_g t), \quad (\text{A2})$$

where the superscript zero refers to the activity at the end of an irradiation, and  $q$  is the ratio of decay constants  $\lambda_g/(\lambda_g - \lambda_m)$ .

The observed counting rate  $R_m$  attributable to  $^{137m}\text{Ce}$  is

$$R_m = k c_m A_m, \quad (\text{A3})$$

where  $k$  is a counting efficiency which includes a geometrical factor, external absorption loss, self-absorption loss, scattering, intrinsic efficiency of the proportional counter for 5-keV radiation, etc.;  $c_m$  is the fraction of decay events of  $^{137m}\text{Ce}$  which leads to the emission of Ce  $L$  x rays. It is given by

$$c_m = \omega_L [\alpha_L^m / (\alpha_T^m + 1) + \omega_K \alpha_K^m / (\alpha_T^m + 1) + 1.33(1 - \omega_K) \alpha_K^m / (\alpha_T^m + 1)], \quad (\text{A4})$$

where  $\alpha_L^m$ ,  $\alpha_K^m$ , and  $\alpha_T^m$  are internal-conversion coefficients for the 255-keV isomeric transition, and  $\omega_K$  and  $\omega_L$  are the  $K$ - and  $L$ -shell fluorescence yields. The first term represents  $L$  conversion of the 255-keV transition; the second is the number of  $L$  vacancies per  $K$  vacancy when the latter is de-excited by the emission of a  $K$  x ray. The third indicates the number of  $L$  vacancies per  $K$  vacancy when a  $K$  Auger process occurs. The numerical factor 1.33 is based on the premise that  $(K-LX)/(K-LL)$  is 0.5 in  $^{137}\text{Ce}$ .<sup>33</sup>

Similarly, for the decay of  $^{137g}\text{Ce}$

$$R_g = k c_g A_g. \quad (\text{A5})$$

Two processes contribute here to  $c_g$ : the electron-capture transitions and conversion of the 10-keV  $\gamma$  ray. Hence

$$c_g = \omega_L [f_L + f_K \omega_K + 1.33(1 - \omega_K) f_K + \alpha_L^g / (\alpha_T^g + 1)], \quad (\text{A6})$$

where  $f_L$  and  $f_K$  are the fractions of electron-capture transitions which occur as  $L$  or  $K$  capture; the 3% branch to the 445-keV level is disregarded in our calculations. The conversion coefficients  $\alpha_L^g$  and  $\alpha_T^g$

refer to the 10-keV transition in the decay of the ground state. The second and third terms in square brackets give the contribution of La  $L$  x rays from the de-excitation of a  $K$  vacancy by  $K$  x rays and by the Auger process, respectively.

The observed counting rate  $R$  of the 5-keV photopeak (plus the escape peak in Ar) is given by

$$R = R_m + R_g. \quad (\text{A7})$$

The various constants in Eq. (A4) and (A6) were assumed to be  $\omega_K = 0.90$ ,<sup>33</sup>  $\alpha_L^m / (\alpha_T^m + 1) = 0.22$ ,<sup>23</sup>  $\alpha_K^m / (\alpha_T^m + 1) = 0.65$ ,<sup>23</sup>  $f_K = 0.89$ ,<sup>33</sup>  $f_L = 0.11$ ,<sup>33</sup> and  $\alpha_T^g \approx 140$ .<sup>23</sup> The quantity  $\alpha_L^g / (\alpha_T^g + 1)$  is not known for the 10-keV  $\gamma$  ray, and calculated values of  $\alpha_L^g / \alpha_M^g$  must be extrapolated over a large energy range. The experimental evidence is that  $\alpha_L / \alpha_M$  is typically about 4 and not a sensitive function of multipolarity or of transition energy (if it is large compared to the  $L$ -shell binding energy). This suggests that a reasonable value for  $\alpha_L^g / (\alpha_T^g + 1)$  is  $\approx 0.8$ . Fortunately the isomeric cross-section ratio  $\sigma(^{137m}\text{Ce}) / \sigma(^{137g}\text{Ce})$  is insensitive to the choice of this quantity over the range 0.5 to 1.0. There is disagreement in the literature for the value of  $\omega_L$ <sup>33,34</sup>; however, for calculating isomeric ratios it need not be known.

With these constants Eqs. (A4) and (A6) become

$$c_m = 0.89 \omega_L \quad (\text{A8})$$

and

$$c_g = 1.83 \omega_L. \quad (\text{A9})$$

If we substitute from Eqs. (A1), (A2), (A3), and (A5) into Eq. (A7), multiply both sides of Eq. (A7) by  $\exp(\lambda_g t)$ , and insert numerical values, we obtain

$$R \exp(\lambda_g t) = k \omega_L \{ 3.34 A_m^0 \times [\exp(\lambda_g - \lambda_m) t - 0.73] + 1.83 A_g^0 \}. \quad (\text{A10})$$

A graph of  $R \exp(\lambda_g t)$  against  $\exp(\lambda_g - \lambda_m) t - 0.73$  should be linear with slope  $3.34 A_m^0$  and intercept  $1.83 A_g^0$ , both in units of  $k \omega_L$ . The relationship between  $A_m^0$  and  $A_g^0$  and their corresponding cross sections  $\sigma(^{137m}\text{Ce})$  and  $\sigma(^{137g}\text{Ce})$  is straightforward. In the isomeric cross-section ratio  $\sigma_m / \sigma_g$  the quantity  $k \omega_L$  cancels.

For cross-section calculations we use  $\omega_L = 0.17$ <sup>33</sup> and  $k = 0.049 A_s$  where  $A_s$  is the self-absorption correction and depends on sample thickness. The numerical coefficient in  $k$  was determined by extrapolation from measured efficiencies with thin sources of standard  $^{54}\text{Mn}$  (5.4-keV  $K$  x ray of  $^{54}\text{Cr}$ ) and  $^{65}\text{Zn}$  (8.1-keV  $K$  x ray of  $^{65}\text{Cu}$ ) which were obtained from the National Bureau of Standards.

<sup>33</sup> A. H. Wapstra, G. J. Nijgh, and R. van Lieshout, *Nuclear Spectroscopy Tables* (North-Holland Publishing Company, Amsterdam, 1959), Chap. 7.

<sup>34</sup> K. Hohmuth, G. Mueller, and J. Schintlmeister, Nucl. Phys. 48, 209 (1963).